

# <sup>1</sup> PeriDEM – High-fidelity modeling of granular media consisting of deformable complex-shaped particles

<sup>3</sup> **Prashant K. Jha**  <sup>1</sup>

<sup>4</sup> <sup>1</sup> Department of Mechanical Engineering, South Dakota School of Mines and Technology, Rapid City,  
<sup>5</sup> SD 57701, USA

DOI: [10.xxxxxx/draft](https://doi.org/10.xxxxxx/draft)

## Software

- [Review](#) 
- [Repository](#) 
- [Archive](#) 

Editor: [Open Journals](#) 

Reviewers:

- [@openjournals](#)

Submitted: 01 January 1970

Published: unpublished

## License

Authors of papers retain copyright and release the work under a Creative Commons Attribution 4.0 International License ([CC BY 4.0](#))<sup>17</sup><sup>18</sup>

## <sup>6</sup> Summary

<sup>7</sup> Accurate simulation of granular materials under extreme mechanical conditions, such as crushing,  
<sup>8</sup> fracture, and large deformation, remains a significant challenge in geotechnical, manufacturing,  
<sup>9</sup> and mining applications. Classical discrete element method (DEM) models typically treat  
<sup>10</sup> particles as rigid or nearly rigid bodies, limiting their ability to capture internal deformation and  
<sup>11</sup> fracture. The PeriDEM library, first introduced in ([Jha et al., 2021](#)), addresses this limitation  
<sup>12</sup> by modeling particles as deformable solids using peridynamics, a nonlocal continuum theory  
<sup>13</sup> that naturally accommodates fracture and significant deformation. Inter-particle contact is  
<sup>14</sup> handled using DEM-inspired local laws, enabling realistic interaction between complex-shaped  
<sup>15</sup> particles.

<sup>16</sup> Implemented in C++, PeriDEM is designed for extensibility and ease of deployment. It relies on a minimal set of external libraries, supports multithreaded execution, and includes demonstration examples involving compaction, fracture, and rotational dynamics. The framework facilitates granular-scale simulations, supports the development of constitutive models, and serves as a foundation for multi-fidelity coupling in real-world applications.

## <sup>21</sup> Statement of Need

<sup>22</sup> Granular materials play a central role in many engineered systems, but modeling their behavior under high loading, deformation, and fragmentation remains an open problem. Popular open-source DEM codes such as YADE ([Smilauer et al., 2021](#)), BlazeDEM ([Govender et al., 2016](#)), Chrono DEM-Engine ([Zhang et al., 2024](#)), and LAMMPS ([Thompson et al., 2022](#)) are widely used but typically treat particles as rigid, limiting their accuracy in scenarios involving internal deformation and breakage. A recent review by Dosta et al. ([Dosta et al., 2024](#)) compares several DEM libraries. Meanwhile, peridynamics-based codes such as Peridigm ([Littlewood et al., 2024](#)) and NLMech ([Jha & Diehl, 2021](#)) are designed to simulate deformation and fracture within a single structure, with limited support for multi-structure simulations.

<sup>31</sup> PeriDEM fills this gap by integrating state-based peridynamics for intra-particle deformation with DEM-style contact laws for particle interactions. This hybrid approach enables direct simulation of particle fragmentation, stress redistribution, and dynamic failure propagation—capabilities essential for modeling granular compaction, attrition, and crushing.

<sup>35</sup> Recent multiscale approaches, including DEM-continuum and DEM-level-set coupling methods ([Harmon et al., 2021](#)), aim to bridge scales but often rely on homogenization assumptions. Sand crushing in geotechnical systems, for example, has been modeled using micro-CT-informed FEM or phenomenological laws ([Chen et al., 2023](#)). PeriDEM offers a particle-resolved alternative that allows bottom-up investigation of granular failure and shape evolution, especially in systems where fragment dynamics are critical.

## 41 Background

42 The PeriDEM model was introduced in ([Jha et al., 2021](#)), demonstrating its ability to model  
43 inter-particle contact and intra-particle fracture for complex-shaped particles. It is briefly  
44 described next.

### 45 Brief Introduction to PeriDEM Model

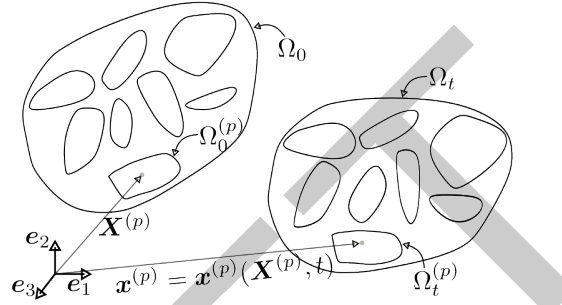


Figure 1: Motion of particle system.

46 Consider a fixed frame of reference and  $\{e_i\}_{i=1}^d$  are orthonormal bases. Consider a collection  
47 of  $N_P$  particles  $\Omega_0^{(p)}$ ,  $1 \leq p \leq N_P$ , where  $\Omega_0^{(p)} \subset \mathbb{R}^d$  with  $d = 2, 3$  represents the initial  
48 configuration of particle  $p$ . Suppose  $\Omega_0 \supset \cup_{p=1}^{N_P} \Omega_0^{(p)}$  is the domain containing all particles; see  
49 [Figure 1](#). The particles in  $\Omega_0$  are dynamically evolving due to external boundary conditions and  
50 internal interactions; let  $\Omega_t^{(p)}$  denote the configuration of particle  $p$  at time  $t \in (0, t_F]$ , and  
51  $\Omega_t \supset \cup_{p=1}^{N_P} \Omega_t^{(p)}$  domain containing all particles at that time. The motion  $x^{(p)} = x^{(p)}(\mathbf{X}^{(p)}, t)$   
52 takes point  $\mathbf{X}^{(p)} \in \Omega_0^{(p)}$  to  $x^{(p)} \in \Omega_t^{(p)}$ , and collectively, the motion is given by  $x = x(\mathbf{X}, t) \in$   
53  $\Omega_t$  for  $\mathbf{X} \in \Omega_0$ . We assume the media is dry and not influenced by factors other than  
54 mechanical loading (e.g., moisture and temperature are not considered). The configuration of  
55 particles in  $\Omega_t$  at time  $t$  depends on various factors, such as material and geometrical properties,  
56 contact mechanism, and external loading. Essentially, there are two types of interactions  
57 present in the media:

- 58     ▪ *Intra-particle interaction* that models the deformation and internal forces in the particle  
59       and
- 60     ▪ *Inter-particle interaction* that accounts for the contact between particles and the boundary  
61       of the domain in which the particles are contained.

62 In DEM, the first interaction is ignored, assuming that particle deformation is insignificant  
63 compared to inter-particle interactions. On the other hand, PeriDEM accounts for both  
64 interactions.

65 The balance of linear momentum for particle  $p$ ,  $1 \leq p \leq N_P$ , takes the form:

$$\rho^{(p)} \ddot{\mathbf{u}}^{(p)}(\mathbf{X}, t) = \mathbf{f}_{int}^{(p)}(\mathbf{X}, t) + \mathbf{f}_{ext}^{(p)}(\mathbf{X}, t), \quad \forall (\mathbf{X}, t) \in \Omega_0^{(p)} \times (0, t_F), \quad (1)$$

66 where  $\rho^{(p)}$ ,  $\mathbf{f}_{int}^{(p)}$ , and  $\mathbf{f}_{ext}^{(p)}$  are density, and internal and external force densities. The  
67 above equation is complemented with initial conditions,  $\mathbf{u}^{(p)}(\mathbf{X}, 0) = \mathbf{u}_0^{(p)}(\mathbf{X})$ ,  $\dot{\mathbf{u}}^{(p)}(\mathbf{X}, 0) =$   
68  $\dot{\mathbf{u}}_0^{(p)}(\mathbf{X})$ ,  $\mathbf{X} \in \Omega_0^{(p)}$ .

69 Internal force - State-based peridynamics

70 The internal force term  $f_{int}^{(p)}(\mathbf{X}, t)$  in the momentum balance governs intra-particle deformation  
71 and fracture. In PeriDEM, this term is modeled using a simplified state-based peridynamics for-  
72 mulation that accounts for nonlocal interactions over a finite horizon. The specific constitutive  
73 structure used—including damage-driven bond weakening, volumetric strain contributions, and  
74 neighbor-weighted quadrature—is discussed in detail in (Jha et al., 2021, sec. 2.1 and 2.3).  
75 This formulation allows unified simulation of deformation and fracture in individual particles.

76 DEM-inspired contact forces

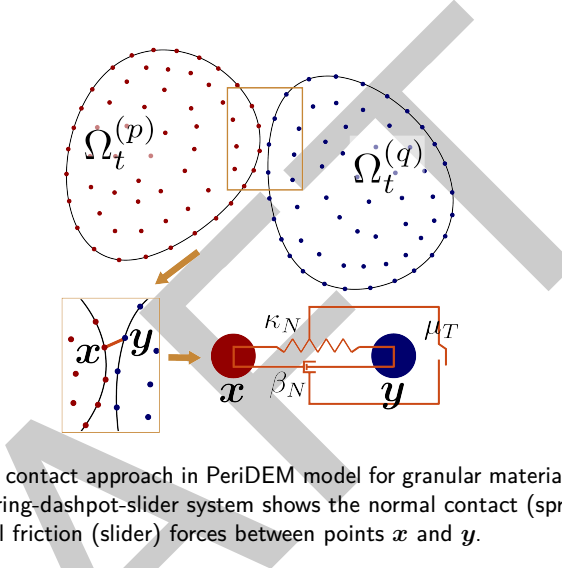


Figure 2: High-resolution contact approach in PeriDEM model for granular materials? between arbitrarily-shaped particles. The spring-dashpot-slider system shows the normal contact (spring), normal damping (dashpot), and tangential friction (slider) forces between points  $x$  and  $y$ .

77 The external force term  $f_{ext}^{(p)}(\mathbf{X}, t)$  includes body forces, wall-particle interactions, and contact  
78 forces from other particles. Contact is modeled using a spring-dashpot-slider formulation applied  
79 locally when particles come within a critical distance. This approach introduces nonlinear normal  
80 forces, damping, and friction without relying on particle convexity or simplified geometries.  
81 Figure 2 illustrates the local high-resolution contact approach between deformable particles.  
82 The full formulation of contact detection, force assembly, and its implementation is provided  
83 in (Jha et al., 2021, sec. 2.2).

84 Implementation

85 PeriDEM is implemented in C++ and hosted on GitHub. It depends on a minimal set of  
86 external libraries, most of which are bundled in the external directory. Some of the key  
87 dependencies include Taskflow (Huang et al., 2021) for multithreaded parallelism, nanoflann  
88 (Blanco & Rai, 2014) for efficient neighborhood search, and VTK for output and post-processing.  
89 The numerical strategies for neighbor search, peridynamic integration, damage evaluation,  
90 and time stepping follow those introduced in (Jha et al., 2021, sec. 3), where additional  
91 implementation details and validation are discussed. The core simulation model is implemented  
92 in `src/model/dem`, with the class `DEMModel` managing particle states, force calculations, and  
93 time integration.

94 This work builds on earlier research in the analysis and numerical methods for peridynamics;  
95 see (Jha & Lipton, 2018a, 2018b, 2019; Jha & Lipton, 2020; Lipton et al., 2019).

## 96 Features

- 97     ▪ Combines peridynamics and DEM to model intra-particle deformation and inter-particle
- 98         contact
- 99
- 100     ▪ Simulates deformation and breakage of single particles under complex loading conditions
- 101
- 102     ▪ Supports arbitrarily shaped particles for realistic granular systems
- 103
- 104     ▪ Ongoing development of MPI-based parallelism and adaptive modeling strategies to
- 105         improve efficiency without sacrificing accuracy

## 106 Examples

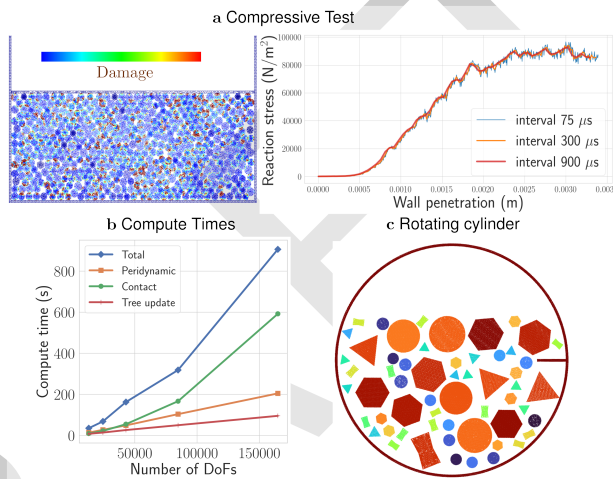


**Figure 3:** (a) Nonlinear response under compression, (b) exponential growth of compute time due to nonlocality of internal and contact forces, and (c) rotating cylinder with nonspherical particles.

107 Example cases are described in [examples/README.md](#). One key simulation demonstrates  
 108 the compression of over 500 circular and hexagonal particles in a rectangular container by  
 109 displacing the top wall. The stress on the wall becomes increasingly nonlinear with penetration  
 110 depth as damage accumulates and the medium yields (see [Figure 3a](#)).

111 Preliminary performance tests show that compute time increases exponentially with particle  
 112 count due to the nonlocal nature of both peridynamic and contact interactions—highlighting  
 113 a computational bottleneck. This motivates future integration of MPI-based parallelism and  
 114 a multi-fidelity modeling framework. Additional examples include attrition of non-circular  
 115 particles in a rotating cylinder ([Figure 3c](#)).

## 116 Acknowledgements

117 This work was supported by the U.S. National Science Foundation through the Engineering  
 118 Research Initiation (ERI) program under Grant No. 2502279. The support has contributed to  
 119 the continued development and enhancement of the PeriDEM library.

## 120 References

- 121 Blanco, J. L., & Rai, P. K. (2014). *Nanoflann: A C++ header-only fork of FLANN, a library*  
 122 *for nearest neighbor (NN) with KD-trees.* <https://github.com/jlblancoc/nanoflann>.

- 123 Chen, Q., Li, Z., Dai, Z., Wang, X., Zhang, C., & Zhang, X. (2023). Mechanical behavior and  
 124 particle crushing of irregular granular material under high pressure using discrete element  
 125 method. *Scientific Reports*, 13(1), 7843.
- 126 Dosta, M., André, D., Angelidakis, V., Caulk, R. A., Celigueta, M. A., Chareyre, B., Dietiker, J.-  
 127 F., Girardot, J., Govender, N., Hubert, C., & others. (2024). Comparing open-source DEM  
 128 frameworks for simulations of common bulk processes. *Computer Physics Communications*,  
 129 296, 109066.
- 130 Govender, N., Wilke, D. N., & Kok, S. (2016). Blaze-DEMGPU: Modular high performance  
 131 DEM framework for the GPU architecture. *SoftwareX*, 5, 62–66.
- 132 Harmon, J. M., Karapiperis, K., Li, L., Moreland, S., & Andrade, J. E. (2021). Modeling  
 133 connected granular media: Particle bonding within the level set discrete element method.  
 134 *Computer Methods in Applied Mechanics and Engineering*, 373, 113486.
- 135 Huang, T.-W., Lin, D.-L., Lin, C.-X., & Lin, Y. (2021). Taskflow: A lightweight parallel and  
 136 heterogeneous task graph computing system. *IEEE Transactions on Parallel and Distributed  
 137 Systems*, 33(6), 1303–1320. <https://doi.org/10.1109/TPDS.2021.3104255>
- 138 Jha, P. K., Desai, P. S., Bhattacharya, D., & Lipton, R. (2021). Peridynamics-based discrete  
 139 element method (PeriDEM) model of granular systems involving breakage of arbitrarily  
 140 shaped particles. *Journal of the Mechanics and Physics of Solids*, 151, 104376. <https://doi.org/10.1016/j.jmps.2021.104376>
- 142 Jha, P. K., & Diehl, P. (2021). NLMech: Implementation of finite difference/meshfree  
 143 discretization of nonlocal fracture models. *Journal of Open Source Software*, 6(65), 3020.  
 144 <https://doi.org/10.21105/joss.03020>
- 145 Jha, P. K., & Lipton, R. (2018a). Numerical analysis of nonlocal fracture models in holder  
 146 space. *SIAM Journal on Numerical Analysis*, 56(2), 906–941. <https://doi.org/10.1137/17M1112236>
- 148 Jha, P. K., & Lipton, R. (2018b). Numerical convergence of nonlinear nonlocal continuum  
 149 models to local elastodynamics. *International Journal for Numerical Methods in Engineering*,  
 150 114(13), 1389–1410. <https://doi.org/10.1002/nme.5791>
- 151 Jha, P. K., & Lipton, R. (2019). Numerical convergence of finite difference approximations for  
 152 state based peridynamic fracture models. *Computer Methods in Applied Mechanics and  
 153 Engineering*, 351, 184–225. <https://doi.org/10.1016/j.cma.2019.03.024>
- 154 Jha, P. K., & Lipton, R. P. (2020). Kinetic relations and local energy balance for LEFM from  
 155 a nonlocal peridynamic model. *International Journal of Fracture*. <https://doi.org/10.1007/s10704-020-00480-0>
- 157 Lipton, R. P., Lehoucq, R. B., & Jha, P. K. (2019). Complex fracture nucleation and evolution  
 158 with nonlocal elastodynamics. *Journal of Peridynamics and Nonlocal Modeling*, 1(2),  
 159 122–130. <https://doi.org/10.1007/s42102-019-00010-0>
- 160 Littlewood, D. J., Parks, M. L., Foster, J. T., Mitchell, J. A., & Diehl, P. (2024). The  
 161 peridigm meshfree peridynamics code. *Journal of Peridynamics and Nonlocal Modeling*,  
 162 6(1), 118–148.
- 163 Smilauer, V., Angelidakis, V., Catalano, E., Caulk, R., Chareyre, B., Chèvremont, W., Doro-  
 164 feenko, S., Duriez, J., Dyck, N., Elias, J., Er, B., Eulitz, A., Gladky, A., Guo, N., Jakob, C.,  
 165 Kneib, F., Kozicki, J., Marzougui, D., Maurin, R., ... Yuan, C. (2021). Yade documentation  
 166 (3rd edition). *Zenodo*. <https://doi.org/10.5281/zenodo.5705394>
- 167 Thompson, A. P., Aktulga, H. M., Berger, R., Bolintineanu, D. S., Brown, W. M., Crozier, P.  
 168 S., in 't Veld, P. J., Kohlmeyer, A., Moore, S. G., Nguyen, T. D., Shan, R., Stevens, M. J.,  
 169 Tranchida, J., Trott, C., & Plimpton, S. J. (2022). LAMMPS - a flexible simulation tool for  
 170 particle-based materials modeling at the atomic, meso, and continuum scales. *Computer*

<sup>171</sup>      *Physics Communications*, 271, 108171. <https://doi.org/https://doi.org/10.1016/j.cpc.2021.108171>

<sup>173</sup>      Zhang, R., Tagliafierro, B., Vanden Heuvel, C., Sabarwal, S., Bakke, L., Yue, Y., Wei, X.,  
<sup>174</sup>      Serban, R., & Negruț, D. (2024). Chrono DEM-Engine: A discrete element method  
<sup>175</sup>      dual-GPU simulator with customizable contact forces and element shape. *Computer Physics Communications*, 300, 109196. <https://doi.org/https://doi.org/10.1016/j.cpc.2024.109196>

DRAFT